Electron Transport in Disordered Graphene Nanoribbons

Melinda Y. Han,[1] Juliana C. Brant,[1,2] and Philip Kim[1]

[1]*Department of Physics and Department of Applied Physics, Columbia University, New York, New York 10027, USA*
[2]*Departamento de Física, Universidade Federal de Minas Gerais, Belo Horizonte, Minas Gerais 30123-970, Brazil*

We report an electron transport study of lithographically fabricated graphene nanoribbons (GNRs) of various widths and lengths. At the charge neutrality point, a length-independent transport gap forms whose size is inversely proportional to the GNR width. In this gap, electrons are localized, and charge transport exhibits a transition between thermally activated behavior at higher temperatures and variable range hopping at lower temperatures. By varying the geometric capacitance, we find that charging effects constitute a significant portion of the activation energy.

PACS numbers: 73.23.−b, 85.35.−p

In recent years graphene has been celebrated for its potential as a new electronic material [1,2]. However, the absence of an energy band gap in graphene poses a challenge for conventional semiconductor device operations. Previous work [3–5] has shown that this hurdle can be overcome by patterning graphene into nanometer size ribbons or constrictions. The resulting transport gap formation can be most simply attributed to quasi-one-dimensional (1D) confinement of the carriers, which induces an energy gap in the single particle spectrum [6]. Detailed experimental studies of disordered graphene nanoribbons (GNRs) [7–12], however, suggest that this observed transport gap may not be a simple band gap. In an effort to explain these experimental results, various theoretical explanations for the transport gap formation in disordered graphene nanostructures have been proposed, including models based on Coulomb blockade in a series of quantum dots [13], Anderson localization due to edge disorder [14–19], and a percolation driven metal-insulator transition [20]. In order to distinguish between these different scenarios, systematic experiment including treatment of both disorder induced localization and electron-electron interaction is required.

In this Letter, we study the scaling of the transport gap in GNRs of various dimensions. From the scaling of several characteristic energies with GNR width (W) and length (L), we find evidence of a transport mechanism in disordered GNRs based on hopping through localized states whose size is close to the GNR width.

GNRs were fabricated following the procedures described in [3]. Most experiments in this report were performed on back-gated GNRs on a substrate of highly doped silicon with a 285 nm thick SiO_2 gate dielectric. An example of such a device is shown in the inset to Fig. 1(a). We measured electron transport in a total of 41 GNRs with $20 < W < 120$ nm and $0.5 < L < 2$ μm. Additionally, we fabricated top-gated GNRs with 15 nm of hydrogen silsesquioxane (HSQ) and 10 nm of HfO_2 as the gate dielectric material for a comparative study.

GNR conductance is strongly suppressed for a region of back gate voltages V_g near the graphene charge neutrality point [3,4,8–12], suggesting the formation of a transport gap. Figure 1(a) shows low bias differential conductance $G = dI/dV$ as a function of V_g for a typical GNR. The transport gap region as measured in back gate voltage, ΔV_g, can be identified in this curve by extrapolating the
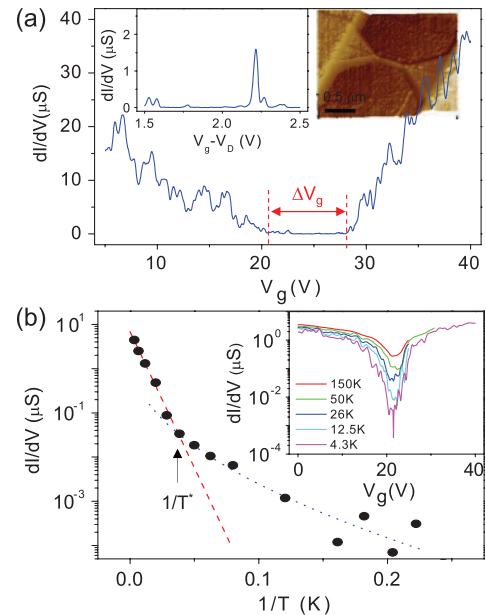

FIG. 1 (color online). (a) dI/dV of a GNR with $W = 36$ nm and $L = 500$ nm, plotted as a function of V_g. Dashed lines highlight measurement of ΔV_g. Right inset shows an atomic force microscope image of the device. Left inset shows a close-up of dI/dV within the gap regime plotted as a function of $V_g - V_D$, where $V_D = 21$ V is the gate voltage for the charge neutrality point. (b) T dependence of the minimum conductance of the same GNR in (a). The dashed and dotted lines are a fit to simple activated behavior and variable range hopping with $\gamma = 1/2$, respectively. An arrow highlights the position of T^*. Inset shows $dI/dV(V_g)$ at several temperatures.

smoothed dG/dV_g to zero [8,12]. We note that reproducible conductance peaks appear in the gap region [8,9,12] [left inset Fig. 1(a)], which are indicative of resonant conduction paths through localized states inside the transport gap. In general, resonance peaks in the gap are less than 10% of the G values outside of the gap region.

The observed transport gap, ΔV_g corresponds to an energy in the single particle energy spectrum: $\Delta_m = \hbar v_F \sqrt{2\pi C_g \Delta V_g / |e|}$, where $v_F = 10^6$ m/sec is the Fermi velocity of graphene [21] and C_g is the capacitive coupling of the GNR to the back gate. This geometric capacitance is strongly dependent on ribbon dimensions and we calculate it using a finite element model, obtaining, for example, $C_g = 690$ aF/μm^2 and $\Delta_m = 200$ meV for the particular device in Fig. 1.

Away from the small resonant conductance peaks, the conductance is strongly suppressed in the transport gap, and the dominant charge transport can be described by thermally excited hopping between localized states. We study the thermal activation of the off-resonant conduction in this regime by measuring $G_{\min}$, the minimum conductance for a given sweep of gate voltage V_g, at different temperatures [inset to Fig. 1(b)]. Figure 1(b) shows an Arrhenius plot for $G_{\min}(T)$. Evidently, thermally excited transport exhibits two distinct behaviors at low and high temperature regimes, respectively, separated by a characteristic temperature T^*. At high temperatures ($T > T^*$), the transport is simply activated: $G_{\min} \sim \exp(-E_a/2k_B T)$, where $E_a = 285$ K is obtained from a linear fit of the Arrhenius plot (dashed line). At lower temperatures ($T < T^*$), however, $G_{\min}$ deviates from the simple activation behavior and decreases more slowly with decreasing temperature than the activated transport would imply. In this low temperature regime, the overall behavior is consistent with variable range hopping (VRH), where $G \sim \exp(-(T_0/T)^\gamma)$, with $\gamma = 1/2$ and a constant T_0, determined by the characteristics of the localized states [22].

The aforementioned GNR transport gap and temperature dependent characteristics are typical of all GNRs with $W \lesssim 80$ nm, so that Δ_m, E_a, and $k_B T^*$ can be determined for each of these narrow GNRs. These three representative energy scales are plotted as a function of W in Fig. 2. In this graph, we note that (i) there is a clear separation between these energy scales, setting a general relation $\Delta_m > E_a > k_B T^*$ for given W, (ii) Δ_m, E_a, and T^* depend sensitively on W but not L, and (iii) the energy scales are reasonably well described by inverse proportion to the lateral confinement of the GNR. The length independence can be noticed by comparing characteristic energies of the GNRs with similar W but different L (represented by different symbols in Fig. 2), and suggests that these three energy scales are 1D intensive properties of GNRs. To show this, we define the normalized width $w = (W - W_0)/a_0$, where $a_0 = 0.142$ nm is the carbon-carbon bond length and W_0 is an
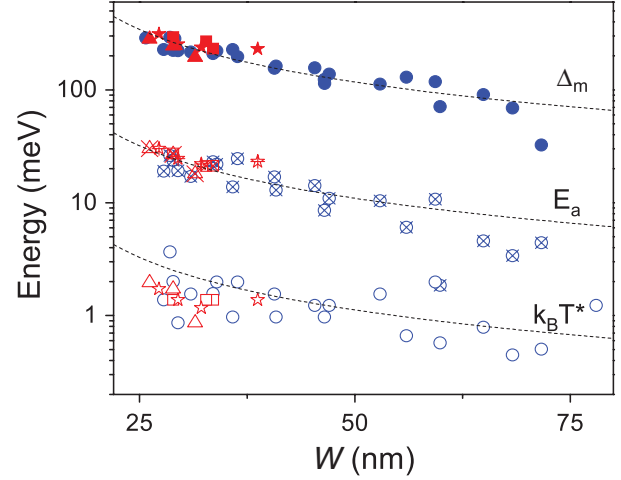

FIG. 2 (color online). GNR transport energy scales: Δ_m (solid), E_a (crosshatched), and $k_B T^*$ (open) plotted as a function of GNR width. Circles, triangles, squares, and stars correspond to ribbons of $L = 0.5$, 1, 1.5, and 2 μm, respectively. The dashed lines are the fits described in the text.

offset introduced phenomenologically. Then, we find that all energy scales can be reasonably fit (dotted lines): $\Delta_m = \Delta_m^0/w$; $E_a = E_a^0/w$; $T^* = T_0^*/w$ with the proportionality parameters $\Delta_m^0 = 36.3$ eV, $E_a^0 = 3.39$ eV, and $k_B T_0^* = 347$ meV, respectively, with $W_0 = 12$ nm held fixed for all three fits [23].

Edge disorder in the GNRs tends to induce wave function localization, with a localization length that decreases rapidly with decreasing energy, resulting in a transport gap with strongly localized states at energies between the mobility edges [14]. The size of this mobility gap is larger than the clean band gap of an ideal ribbon; Querlioz *et. al.* calculate the scaling prefactor $\Delta_m^0 \approx 32.2$ eV, averaged over many configurations of edge disorder [17]. The close match of our data to theoretical prediction supports the view that atomic defects at the graphene edges create localized states. We point out, however, that the observed energy scales lie within the range of the disorder potential fluctuation created by charged impurities in the SiO$_2$ substrate [20], making it difficult to exclude the contribution of a substrate disorder induced transport gap, as discussed in a recent experiment on transport in thermally annealed GNRs [12].

On the other hand, $E_a^0/\Delta_m^0 \approx 0.1$; i.e., the activation energy at higher temperatures is an order of magnitude smaller than Δ_m. This observation excludes the scenario that extended states carry current via thermal activation across the transport gap. Instead, we interpret the simply activated behavior as a signature of 1D nearest neighbor hopping (NNH) through localized states within the transport gap [19]. In this picture, disorder at the edges tends to produce a rapid variation in the local density of states over the whole width of the ribbon, blocking the conductive paths and leading to a quasi-1D arrangement of localized

states [16]. Martin and Blanter predict [19] that the energy spacing between nearest neighbor states is determined by $\sim t'/w$, where $t' \approx 0.2t$ is the hopping matrix element between second nearest neighbor carbon atoms in graphene, so that $E_a^0 \sim 2t' = 1.2$ eV. Our measured value for this scaling prefactor, 3.39 eV, is somewhat larger than this prediction, which may be explained by the contribution of a charging energy to the hopping energy E_a, discussed in more detail below.

The change of the transport behavior across the temperature T^* allows a further comparison of our data to theory. In a very recent theoretical work, the NNH and VRH crossover is calculated to occur at $T^* = E_a/k_B\alpha$, where $\alpha \approx 8$ was estimated numerically [24]. In our experiment, we obtain $E_a^0/k_B T_0^* = 9.8$, reasonably consistent with this theoretical prediction, lending further support to a model of charge transport via thermally activated hopping between localized states.

An alternative approach to probing the GNR transport gap is measurement of the nonlinear transport characteristics [3]. Figure 3(a) shows differential conductance, dI/dV_b as a function of V_g and source-drain bias voltage V_b. Transport through the GNR at finite V_b shows a strong nonlinear $I - V_b$ characteristic when E_F is in the transport gap regime, which is most extreme when V_g is near the charge neutrality point of the GNR [Fig. 3(b), black curve].
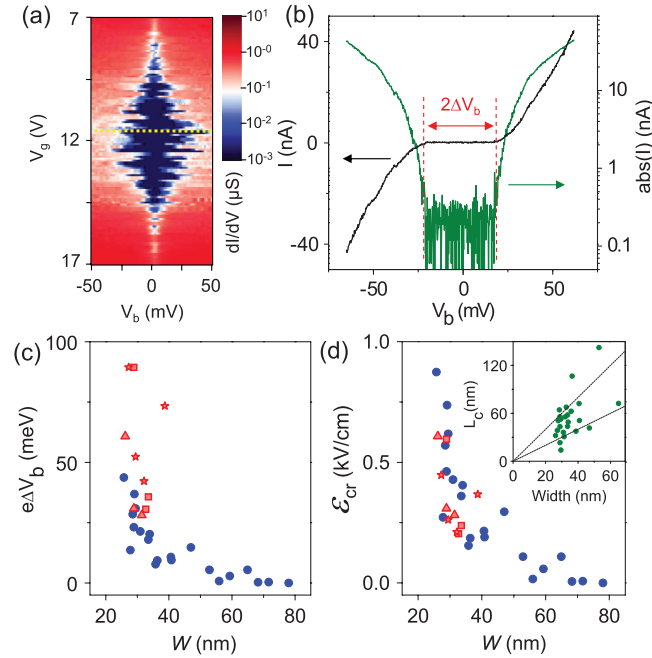
The nonlinear gap ΔV_b can be defined where a steep increase of current appears in logarithmic scale [Fig. 3(b), green (dark gray) curve].

In our previous study [3], the energy corresponding to $e\Delta V_b$ was interpreted to be the band gap of the GNR. However, this naive interpretation should be carefully reconsidered for edge disordered GNRs, where the charge transport is dominated by hopping through localized states. Indeed, from the plot of ΔV_b vs W [Fig. 3(c)], we notice that ΔV_b depends strongly on L, and is not well determined by W alone, unlike the previous three characteristic energy scales (Δ_m, E_a, and $k_B T^*$). Since the charge transport in the disordered GNRs is diffusive, it is likely that electric field is driving transport in the transport gap. Indeed, if we convert ΔV_b into the corresponding critical electric field $\mathcal{E}_{cr} = \Delta V_b/L$, we restore a reasonable scaling behavior, where $\mathcal{E}_{cr}$ depends only on W and not on L [Fig. 3(d)].

In disordered systems in which transport is dominated by hopping through localized states, applied electric field $\mathcal{E}$ plays a similar role to temperature. Thus we can treat the electric field as an effective temperature: $k_B T_{eff} = e\mathcal{E}L_c$, where L_c is the averaging hopping length between localized states [25]. Noting that the transition from NNH dominated transport to VRH transport occurs at T^*, we relate T^* to the transition occurring at $\mathcal{E}_{cr}$ and estimate $L_c \approx k_B T^*/e\mathcal{E}_{cr}$. For most GNRs in this experiment we find that $W \lesssim L_c < 2W$ [Fig. 3(d) inset]. The fact that $L_c \gtrsim W$ supports our claim that hopping transport through the ribbons is effectively 1D. We note that this L_c is distinct from the wave function localization length, which should be smaller than L_c and is expected to be comparable to W [26,27].

FIG. 3 (color online).   (a) Differential conductance as a function of V_g and V_b measured in a GNR with $L = 1$ μm and $W = 31$ nm. (b) Current as a function of V_b with V_g fixed in the off-resonant condition marked by the dotted line in (a). ΔV_b is highlighted by the vertical dashed lines. (c) ΔV_b as a function of W. Symbols follow the convention set in Fig. 2. (d) The critical electric field $\mathcal{E}_{cr}$ versus W converted from the data set in (c).

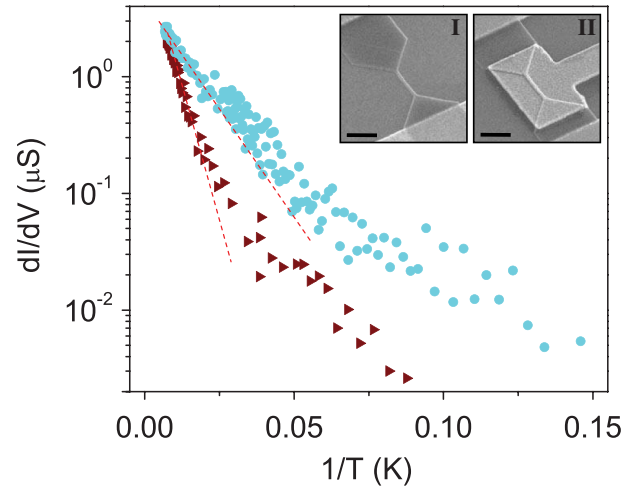
FIG. 4 (color online).   Temperature dependence of the conductance minimum for dual gated (circles) and back gated (triangles) GNRs with the similar W and L. The dashed lines are Arrhenius fits in the high temperature regime. The inset shows SEM images of back gated (left) and dual gated (right) devices. Scale bar represents 500 nm.

Finally, we discuss the effect of Coulomb charging in GNRs. Several previous works have discussed the role of Coulomb blockade and charging effects on the transport gap in GNRs and graphene constrictions [8,12,13]. In principle, in a GNR with hopping between localized states, we expect Coulomb interactions to open a soft Coulomb gap near the Fermi surface, which can be incorporated into the total hopping energy E_a in addition to the single particle energy level spacing t'/w, so that $E_a \approx t'/w + E_c$, where E_c is the Coulomb charging energy [19,28,29]. In order to quantify the contribution of charging energy E_c to the hopping energy E_a, we perform a comparative transport measurement on GNRs with different gate coupling. Figure 4 shows the temperature dependent minimum conductance $G_{\min}(T)$ for a back gate only GNR (device I) and a GNR with both top and back gates (device II) with similar W and L. While device I has the usual capacitive coupling to the back gate, (i.e., $C^I \approx C_g$), device II is much closer to the top gate, leading to a larger capacitance: $C^{II}/C^I \approx 4$. From the thermally activated Arrhenius behavior in the high temperature regime (dashed lines), we obtain the activation energies of the two devices, $E_a^I = 15$ meV and $E_a^{II} = 8.4$ meV averaged over two devices of type I and four of type II. Considering the reduced charging energy contribution in the dual gated device, smaller values of the activation energy are indeed expected, if Coulomb effects are appreciable in the GNR.

Employing the ratio $E_a^{II}/E_a^I \approx 0.5$, we now can estimate the charging energy contribution quantitatively. Assuming that the single particle energy level spacing t'/w is similar for both GNRs due to their similar dimensions, we obtain $E_a^{II} - E_c^{II} = E_a^I - E_c^I = t'/w$, where the charging energy ratio of device I and II are given by $E_c^I/E_c^{II} = C^{II}/C^I \approx 4$. The resulting estimate for the charging energy contribution, $E_c^I/E_a^I \approx 0.6$, indicates that the Coulomb charging effect provides a substantial portion of the activation energy.

In conclusion, we study length and width dependent resistance scaling in GNRs. Temperature and electric field dependent transport characteristics indicate that charge transport in the transport gap of disordered GNRs is dominated by localized states, where the Coulomb charging effects play an important role.

[1] A. K. Geim and K. S. Novoselov, Nature Mater. **6**, 183 (2007).
[2] A. K. Geim and P. Kim, Sci. Am. **298**, 90 (2008).
[3] M. Y. Han *et al.*, Phys. Rev. Lett. **98**, 206805 (2007).
[4] Z. Chen *et al.*, Physica E (Amsterdam) **40**, 228 (2007).
[5] X. Li *et al.*, Science **319**, 1229 (2008).
[6] K. Nakada *et al.*, Phys. Rev. B **54**, 17 954 (1996); K. Wakabayashi *et al.*, Phys. Rev. B **59**, 8271 (1999); M. Ezawa, Phys. Rev. B **73**, 045432 (2006); Y. W. Son, M. L. Cohen, and S. G. Louie, Phys. Rev. Lett. **97**, 216803 (2006); L. Brey and H. A. Fertig, Phys. Rev. B **73**, 235411 (2006); V. Barone, O. Hod, and G. E. Scuseria, Nano Lett. **6**, 2748 (2006).
[7] L. A. Ponomarenko *et al.*, Science **320**, 356 (2008).
[8] C. Stampfer *et al.*, Phys. Rev. Lett. **102**, 056403 (2009).
[9] F. Molitor *et al.*, Phys. Rev. B **79**, 075426 (2009).
[10] K. Todd *et al.*, Nano Lett. **9**, 416 (2009).
[11] X. Liu *et al.*, Phys. Rev. B **80**, 121407(R) (2009).
[12] P. Gallagher, K. Todd and D. Goldhaber-Gordon, arXiv:0909.3886.
[13] F. Sols, F. Guinea, and A. H. CastroNeto, Phys. Rev. Lett. **99**, 166803 (2007).
[14] D. Gunlycke, D. A. Areshkin, and C. T. White, Appl. Phys. Lett. **90**, 142104 (2007).
[15] A. Lherbier *et al.*, Phys. Rev. Lett. **100**, 036803 (2008).
[16] M. Evaldsson *et al.*, Phys. Rev. B **78**, 161407(R) (2008).
[17] D. Querlioz *et al.*, Appl. Phys. Lett. **92**, 042108 (2008).
[18] E. R. Mucciolo, A. H. Castro Neto, and C. H. Lewenkopf, Phys. Rev. B **79**, 075407 (2009).
[19] I. Martin and Y. M. Blanter, Phys. Rev. B **79**, 235132 (2009).
[20] S. Adam *et al.*, Phys. Rev. Lett. **101**, 046404 (2008).
[21] A. H. CastroNeto *et al.*, Rev. Mod. Phys. **81**, 109 (2009).
[22] The hopping length scale can be obtained from the constant T_0. Because of the limited range of measured current, our experimental data it is not sufficient to determine T_0 or the density of states with certainty.
[23] This offset can be ascribed to the critical length scale of the edge localized states [3,16], to the critical percolation length scale [20], or to over-etching underneath the etch mask [3].
[24] A. S. Rodin and M. M. Fogler, Phys. Rev. B **80**, 155435 (2009).
[25] S. Marianer and B. I. Shklovskii, Phys. Rev. B **46**, 13 100 (1992).
[26] G. Schubert, J. Schleede, and H. Fehske, Phys. Rev. B **79**, 235116 (2009).
[27] H. Xu, T. Heinzel, and I. V. Zozoulenko, Phys. Rev. B **80**, 045308 (2009).
[28] M. M. Fogler, S. Teber, and B. I. Shklovskii, Phys. Rev. B **69**, 035413 (2004).
[29] A. L. Efros and B. I. Shklovskii, in *Electron-Electron Interactions in Disordered Systems*, edited by A. L. Efros and M. Pollak (North-Holland, Amsterdam, 1985), p. 409.